Vol. 120: 17–26, 2016
doi: 10.3354/dao03007

DISEASES OF AQUATIC ORGANISMS
Dis Aquat Org

Published June 15

Isolation and preliminary characterization of a new pathogenic iridovirus from redclaw crayfish *Cherax quadricarinatus*

Limei Xu*, Tiantian Wang*, Fang Li, Feng Yang****

Key Laboratory of Marine Genetic Resources, Fujian Collaborative Innovation Center for Exploitation and Utilization of Marine Biological Resources, Third Institute of Oceanography, State Oceanic Administration, Xiamen 361005, PR China

ABSTRACT: We report the preliminary characterization of a new iridovirus detected in diseased *Cherax quadricarinatus* collected from a farm in Fujian, China. Transmission electron microscopy identified numerous icosahedral particles (~150 nm in diameter) in the cytoplasm and budding from the plasma membrane of hematopoietic tissue cells. SDS-PAGE of virions semi-purified from the hemolymph of moribund *C. quadricarinatus* identified 24 proteins including a 50 kDa major capsid protein (MCP). By summing the sizes of DNA restriction endonuclease fragments, the viral genome was estimated to be ~150 kb in length. A 34 amino acid sequence deduced from a 103 bp MCP gene region amplified by PCR using degenerate primers targeted to MCP gene regions conserved among iridoviruses and chloriridoviruses was most similar (55% identity) to Sergestid iridovirus. Based on virion morphology, protein composition, DNA genome length, and MCP sequence relatedness, the virus identified has tentatively been named *Cherax quadricarinatus* iridovirus (CQIV). In addition, experimental infection of healthy *C. quadricarinatus*, *Procambarus clarkii*, and *Litopenaeus vannamei* with CQIV caused the same disease and high mortality, suggesting that CQIV poses a potential threat to cultured and wild crayfish and shrimp.

KEY WORDS: Iridovirus · Crustacean · Ultrastructure · Major capsid protein · Phylogeny

INTRODUCTION

Viruses in the family *Iridoviridae* form large icosahedral virions, possess a linear double-stranded DNA genome and replicate in the cell cytoplasm (Williams et al. 2005, Chinchar et al. 2009). The family currently comprises 5 genera: *Iridovirus*, *Chloriridovirus*, *Lymphocystivirus*, *Ranavirus*, and *Megalocytivirus* (Jancovich et al. 2012). The major capsid protein (MCP) is the most abundant iridovirus structural protein, and as some protein regions are highly conserved, they have been exploited to quantify genome sequence variation among related viruses (Mao et al. 1997, Tang et al. 2007).

Iridoviruses are responsible for many serious diseases in fish, amphibians, and invertebrates (Weissenberg 1965, Anderson 1970, Comps 1988, Marschang et al. 1999, He et al. 2000, Qin et al. 2003). Invertebrate iridoviruses, also known as invertebrate iridescent viruses (IIVs), have mainly been detected in insects and terrestrial isopods. However, there has been 1 report of an IIV infecting a crab (Montanie et al. 1993) and 2 reports of IIVs infecting shrimp (Lightner & Redman 1993, Tang et al. 2007). While these reports inferred infection by IIVs based on virion morphology observed by transmission electron microscopy, the viral genome and/or protein compositions were not investigated.

Here we report the preliminary molecular characterization of a novel iridovirus from cultured redclaw crayfish *Cherax quadricarinatus* named *C. quadricarinatus* iridovirus (CQIV), and its pathogenicity for

*These authors contributed equally to this work
**Corresponding authors: yangfeng5274@163.com; lifang_87@163.com

red swamp crayfish *Procambarus clarkii* and penaeid shrimp *Litopenaeus vannamei*.

MATERIALS AND METHODS

Crustaceans

In 2014, a lethal infectious disease typified by anorexia and lethargy emerged in *Cherax quadricarinatus* being farmed in Fujian, China. Diseased *Cherax quadricarinatus* were collected from an affected farm between July and November 2014. *Procambarus clarkii* (20 g average body weight) and *Litopenaeus vannamei* (10 g average body weight) were purchased from a local market in Xiamen, China. Healthy *C. quadricarinatus* (50 g average body weight) were obtained from Xiamen Xinrongteng Aquatic Technology Development Company. *L. vannamei* were maintained in aerated tanks containing seawater (25‰ salinity) at 25°C. The crayfish were maintained in fresh water at 25°C.

Viral screening

For moribund *C. quadricarinatus*, hemolymph (200 µl) was withdrawn from the base of the fifth pair of walking legs using a 1 ml syringe preloaded with 200 µl anticoagulant solution (26 mM sodium citrate, 30 mM citric acid, 100 mM glucose, 140 mM NaCl, pH 5.8). DNA or RNA was extracted using either a QIAamp DNA Mini Kit (Qiagen) or a High Pure RNA Tissue Kit (Roche), respectively. DNA and RNA were amplified by either PCR or reverse transcription (RT)-PCR to identify the potential presence of white spot syndrome virus (WSSV), infectious hypodermal and hematopoietic necrosis virus (IHHNV), and Taura syndrome virus (TSV). PCR tests were performed according to methods described in the World Organisation for Animal Health Manual of Diagnostic Tests for Aquatic Animals 2015 (www.oie.int/en/international-standard-setting/aquatic-manual/access-online/).

Virion purification

Hemolymph (~40 ml) collected freshly from moribund *C. quadricarinatus* as described above was centrifuged at 1000 × *g* for 5 min to remove hemocytes, and the supernatant was filtered though a 0.2 µm membrane syringe filter to remove bacteria. Virions were then pelleted by centrifugation at 15 000 × *g* for 15 min and resuspended in 0.5 ml TMN buffer (20 mM Tris-HCl pH 7.9, 2 mM $MgCl_2$, 150 mM NaCl).

Transmission electron microscopy (TEM)

The common shrimp viruses WSSV, IHHNV, and TSV were not detected using OIE-endorsed PCR or RT-PCR methods (data not shown), so hematopoietic tissue (HPT) and gill tissues of moribund and healthy *C. quadricarinatus* were examined by TEM. HPT and gill tissue was fixed overnight at 4°C in phosphate-buffered saline containing 1% glutaraldehyde and 4% paraformaldehyde. Tissues were then post-fixed in 1% osmium tetroxide for 12 h, dehydrated stepwise through increasing concentrations of ethanol before being embedded in Epon Resin polymerized at 60°C for 24 h. Tissues were sectioned, stained sequentially with 2% uranyl acetate and 0.4% lead citrate, and visualized using a JEM-1230 transmission electron microscope (JEOL). Suspensions of semi-purified virions were mounted onto formvar-coated, carbon-stabilized copper grids (200 mesh) and negatively stained with 2% sodium phosphotungstate.

Extraction of viral genome DNA

To extract DNA from semi-purified virions, 0.2 ml viral suspension was lysed in 0.8 ml GTE buffer (4 M guanidine isothiocyanate, 20 mM Tris-HCl pH 7.4, 2 mM EDTA). After mixing with an equal volume of isopropanol by inversion, visible white flocculated DNA was transferred into a clean Eppendorf tube and washed twice with 70% ethanol. The DNA was then dissolved in 0.5 ml 0.1× TE buffer (1 mM Tris-HCl pH7.4, 0.1 mM EDTA) containing 0.5% sarcosyl followed by addition of 1 mg ml^{-1} Proteinase K and incubation at 55°C for 2 h. DNA was then extracted with phenol/chloroform and precipitated with isopropanol. After washing twice in 70% ethanol, purified DNA was dissolved in 0.2 ml 0.1× TE buffer and quantified by spectrophotometry.

Restriction endonuclease digestion

Virion DNA (1 µg) was digested separately with 10 U of *Kpn*I, *Eco*RI, *Hin*dIII, *Bam*HI, or *Pst*I in 50 µl reaction volumes at 37°C for 5 h, and DNA fragments were separated in a 0.7% agarose gel electrophoresed at 2 V cm^{-1} for 6 h. DNA bands were stained using ethidium bromide and visualized using a UV

transilluminator. The size of the viral genome was estimated by summing the DNA fragment lengths generated by each restriction endonuclease as deduced from their electrophoretic mobilities (Bächi & Arber 1977, Federici et al. 1990).

Sodium dodecyl sulfate polyacrylamide gel electrophoresis (SDS-PAGE)

Suspensions of semi-purified virions were mixed with an equal volume of 2× Laemmli sample buffer (Laemmli 1970) and boiled for 10 min. Proteins were separated by SDS-PAGE in a 12% gel and visualized by staining with Coomassie brilliant blue R-250.

Cloning of an MCP gene fragment

DNA was extracted from semi-purified virions as well as hemolymph from either moribund or healthy *C. quadricarinatus* using a DNeasy blood and tissue kit (Qiagen). DNA was amplified by PCR using degenerate primers designed for MCP gene regions conserved among iridoviruses and chloriridoviruses (IV-F: 5′-GAA A[C/T])T T[A/T]A TGC ACA ATC TTA T-3′ and IV-R: 5′-CCA ATC AT[A/G] TT[A/G] TC[A/G] TA[C/T] CC-3′). The thermal cycling conditions used were 94°C for 2 min, 25 cycles of 94°C for 30 s, 55°C for 30 s, and 72°C for 30 s, followed by 72°C for 5 min. An aliquot of the PCR product was analyzed by electrophoresis in a 2% agarose gel, and the remainder was used to clone the DNA product. The PCR product nucleotide sequence determined by sequencing 5 clones was translated to deduce its amino acid sequence, which was then used in NCBI BLAST searches (Altschul et al. 1990).

Phylogenetic analysis

The 34 amino acid (aa) MCP region deduced from the cloned PCR product was subjected to Maximum-likelihood analysis using RAxMLGUI 1.5 beta employing the BLOSUM62 model and 1000 rapid bootstrap replicates (Silvestro & Michalak 2012, Stamatakis 2014).

Experimental infections

Healthy batches of *C. quadricarinatus*, *P. clarkii*, and *L. vannamei* were each randomly segregated into 2 groups of 10 individuals and confirmed to be CQIV-free by PCR. Individuals in each group were then injected intramuscularly with 2 µl g^{-1} body weight of either a $1:10^6$ dilution of purified CQIV or sterile normal saline. Mortality was recorded twice daily until no animals remained alive in the infected group. Gill tissues from freshly dead animals were processed for ultrastructural analysis by TEM, and hemolymph was collected from clearly moribund *C. quadricarinatus* to purify virions.

RESULTS

Large icosahedral virus particles present in the cell cytoplasm

In moribund individuals, TEM identified large numbers of virions in the cytoplasm but not the nucleus of HPT cells (Fig. 1a). At higher magnification, the virions were clearly icosahedral and ~150 nm in diameter (Fig. 1b). Frequently, virus particles were also observed budding from the plasma membrane (Fig. 1c) as well as close to and in contact with the inner face of the plasma membrane, surrounded by plasma membrane and budding into the intercellular space at the outer membrane face. Many virions were also observed in the cytoplasm of gill cells of diseased crayfish (Fig. 1e). No virions were observed in either HPT or gill cells of healthy crayfish (Fig. 1d,f). The virus was thus suspected to be the likely cause of disease and mortality in the farmed *C. quadricarinatus*, and based on its morphology, intracellular replication site, and method of cell release, it was suspected to be an iridovirus (Chinchar et al. 2009)

Electron microscopy of negatively-stained virions semi-purified from hemolymph of moribund crayfish by differential centrifugation identified them to be ~155 nm in diameter and to comprise a thin outer shell covering a hexagonal capsid (Fig. 2a).

Virus genome length

In order to estimate the genome length, DNA extracted from semi-purified virions was digested with *Kpn*I, *Eco*RI, *Hin*dIII, *Bam*HI, or *Pst*I, and the resulting DNA fragments were resolved by agarose gel electrophoresis (Fig. 3). By summing the sizes of the fragments generated by each restriction endonuclease relative to the DNA size markers, the viral genome was estimated to be ~150 kb long.

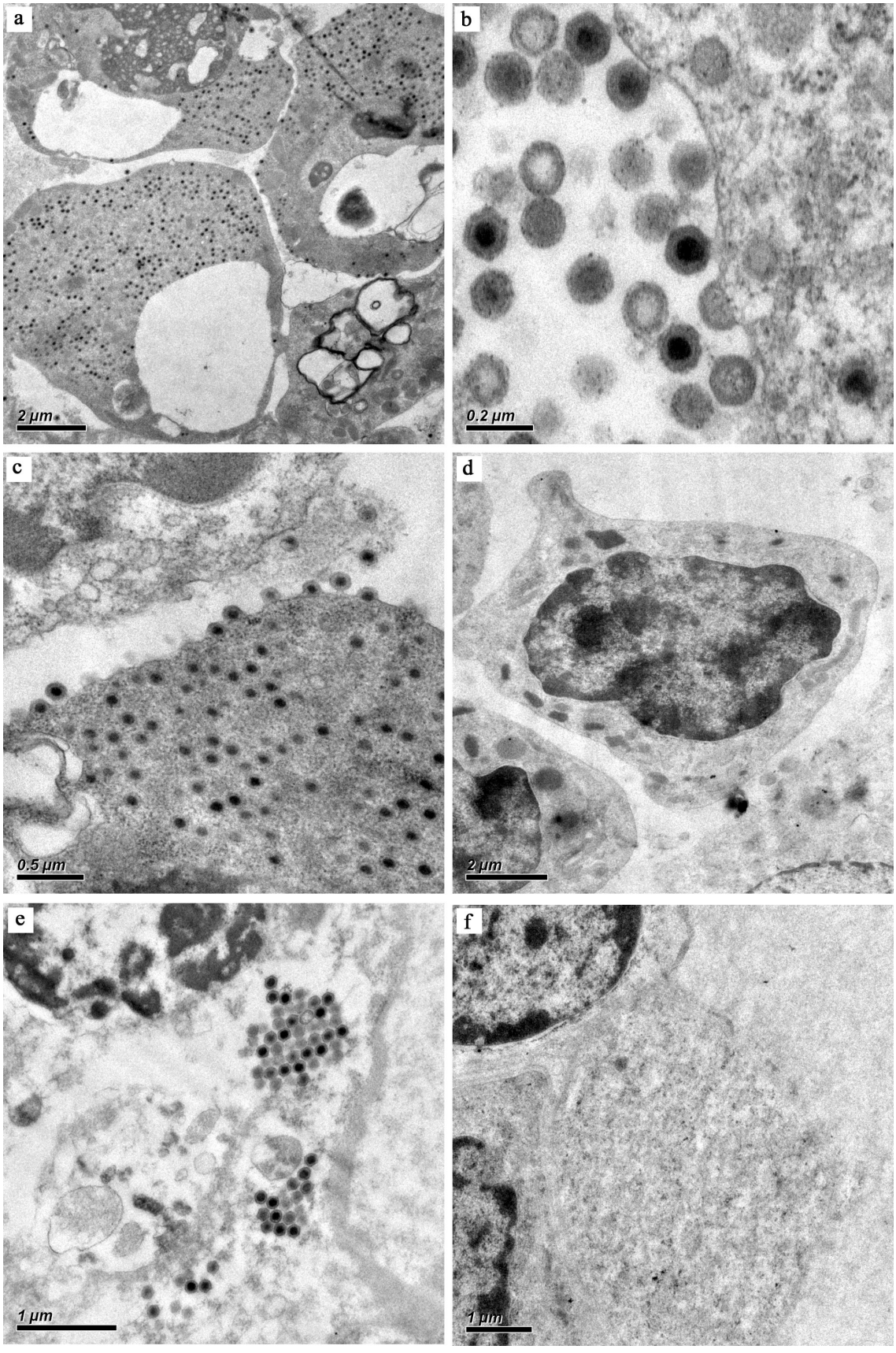

Fig. 1. Transmission electron microscopy (TEM) of diseased *Cherax quadricarinatus* showing large numbers of virions in the cytoplasm of hematopoietic tissue (HPT) cells at (a) low and (b) high magnification, showing virions to be ~150 nm in diameter and hexagonal in shape with an inner dense nucleoid. (c) Virions budding from the HPT plasma membrane into the extracellular space. (e) Virions in the cytoplasm of gill cells. TEM of (d) HPT and (f) gill cells of healthy *C. quadricarinatus*

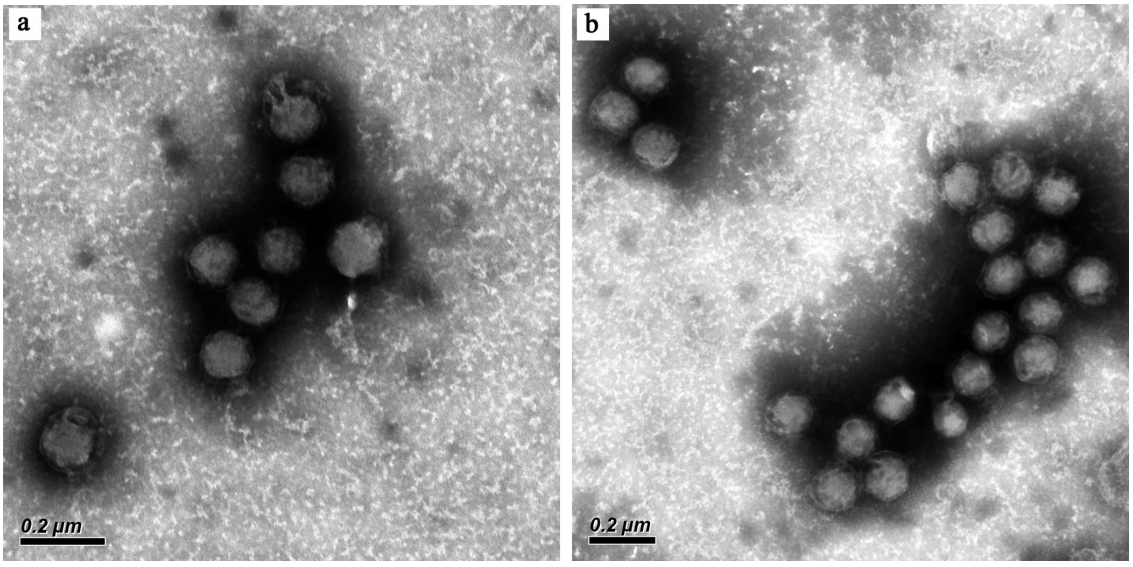

Fig. 2. Transmission electron microscopy of negatively stained virions purified from hemolymph of either (a) naturally or (b) experimentally infected moribund *Cherax quadricarinatus*

Virion protein composition

To examine virus structural protein composition, virions purified from hemolymph of 5 batches of moribund *C. quadricarinatus* collected between July and November 2014 were analyzed by SDS-PAGE (Fig. 4). Protein profiles of the 5 virion preparations were almost identical and comprised 24 more prominent bands including an abundant 50 kDa protein comparable in relative size and abundance to the MCP (48–55 kDa) of iridovirus (Kelly et al. 1979, Jancovich et al. 2012).

CQIV MCP amino acid sequence relatedness to IIV MCPs

To further confirm the identity of the *C. quadricarinatus* virus, a 103 bp region of the MCP gene was amplified using degenerate PCR primers designed for conserved MCP sequences in iridoviruses and chloriridoviruses and DNA extracted from either virions or hemolymph collected from diseased *C. quadricarinatus* (Fig. 5a). Cloning and sequence analysis of the PCR products identified a continuous open reading frame (Fig. 5b). NCBI BLAST analysis identified the 34 aa sequence excluding the primer regions to be most identical (55%) to the MCP of sergestid iridovirus (SIV), between 44 and 48% identical to the MCP of other iridoviruses as well as megalocytivirues and lymphocystiviruses, and slightly less (41%) identical to the MCP of chloriridoviruses (Table 1).

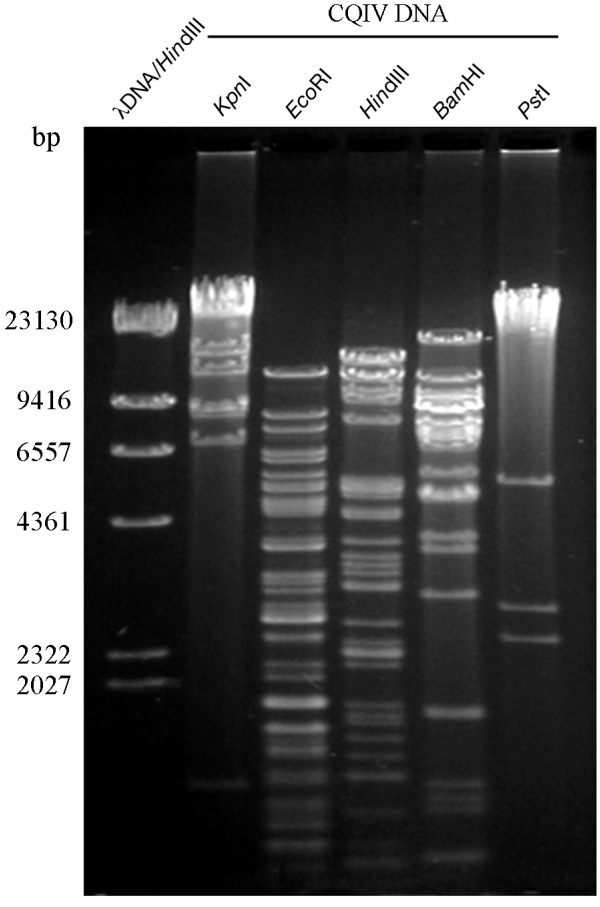

Fig. 3. Agarose gel electrophoresis of DNA extracted from purified *Cherax quadricarinatus* iridovirus (CQIV) following digestion with the restriction endonucleases *Kpn*I, *Eco*RI, *Hin*dIII, *Bam*HI, or *Pst*I

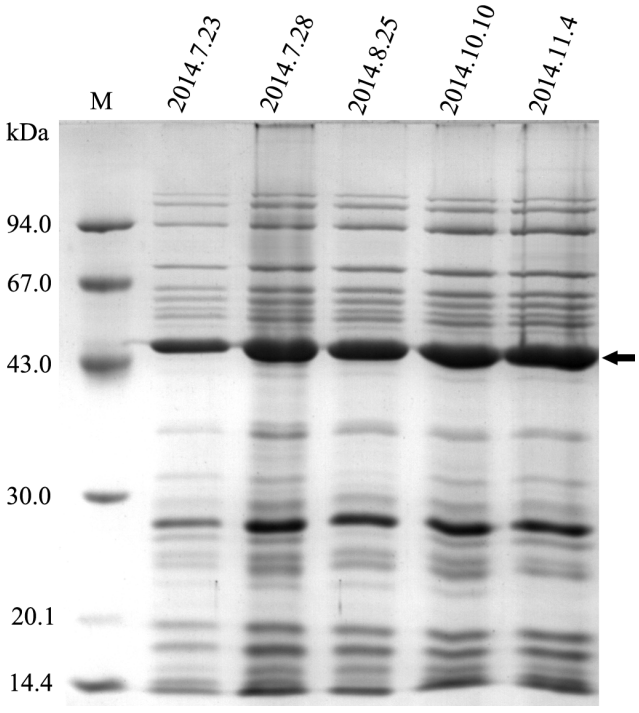

Fig. 4. SDS-PAGE analysis of *Cherax quadricarinatus* iridovirus particles purified from hemolymph collected from 5 batches of naturally infected moribund *C. quadricarinatus* sampled from farms between July and November 2014 (dates given as yr.mo.d). Arrow indicates major capsid protein; Lane M: protein molecular weight markers

Phylogenetic analysis

A maximum-likelihood phylogenetic tree generated using the 34 aa MCP region of iridovirus confirmed CQIV to be distantly related to known invertebrate and vertebrate iridoviruses (Fig. 6). Maximum-likelihood bootstrap values were supported poorly (<60%) for 6 of the 8 clades as a likely result of the very short (34 aa) sequence analyzed. Of the *Iridovirus* species (mean distance 0.9958), the CQIV MCP sequence was closest to SIV (0.76). It was 0.9658 distant from IIV-3 (genus *Chloriridovirus*) and less distant to invertebrate compared to vertebrate iridoviruses, being 1.2548 distant to erythrocytic necrosis virus (ENV; genus *Megalocytivirus*) and having a mean distance of 1.0027 to the members of the genus *Lymphocystivirus*.

Virus pathogenicity for other crustaceans

C. quadricarinatus, *Procambarus clarkii*, and *Litopenaeus vannamei* were injected with either a 10^{-6} dilution of purified CQIV or sterile normal saline. Irrespective of the species, all challenged individuals showed significant gross disease signs such as cessation of feeding and flaccidity at 5 d post-infection (dpi). Mortalities occurred from 9 dpi, and none remained alive at 19 dpi (Fig. 7). No mortalities occurred over this period among the saline-injected controls (data not shown). Mortalities accumulated somewhat more rapidly in *L. vannamei* compared to *C. quadricarinatus* or *P. clarkii*. Among individuals sampled soon after death, virions with characteristic CQIV morphology occurred abundantly in the cytoplasm of gill cells (Fig. 8). Moreover, CQIV was readily isolated from the hemolymph of individuals infected experimentally (Fig. 2b).

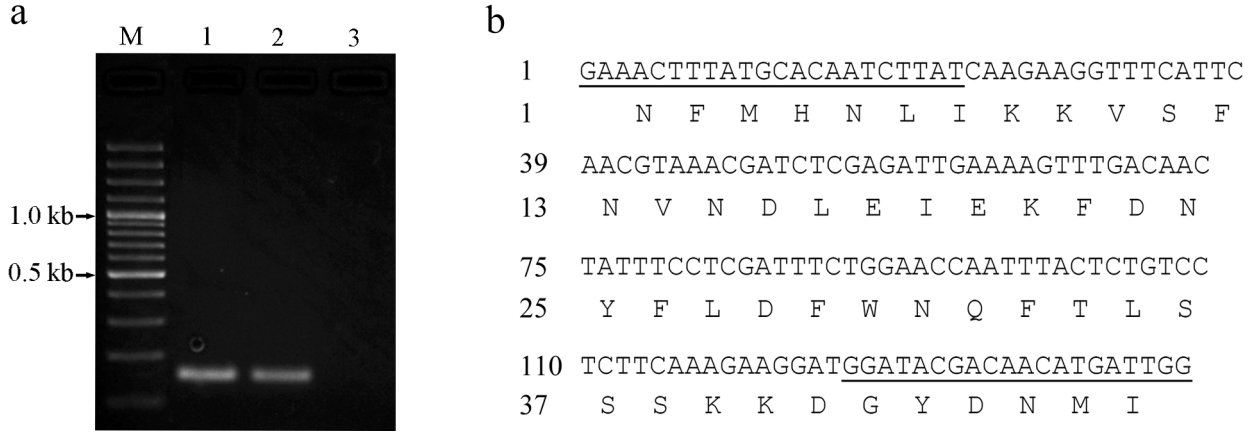

Fig. 5. Major capsid protein (MCP) gene fragment amplified by PCR. (a) Agarose gel electrophoresis of the *Cherax quadricarinatus* iridovirus (CQIV) MCP gene DNA fragment amplified by PCR using DNA extracted from purified virions (Lane 1) and hemolymph of either diseased (Lane 2) or healthy (Lane 3) *C. quadricarinatus*. Lane M: 1 kb DNA ladder. (b) Consensus nucleotide and amino acid sequence deduced from 5 clones of the CQIV MCP gene PCR product (PCR primer sequences underlined)

Table 1. Identity and similarity levels determined for a 34 amino acid (aa) region of the *Cherax quadricarinatus* iridovirus (CQIV) major capsid protein (MCP) sequence

Iridovirus	GenBank accession no.	34 aa CQIV MCP sequence Identical (%)	Similar (%)
Sergestid iridovirus (SIV)	ABR37646.1	18/33 (55)	26/33 (78)
Invertebrate iridescent virus 16 (IIV-16; *Costelytra zealandica* iridescent virus)	O39164.1	16/33 (48)	23/33 (69)
Invertebrate iridescent virus 30 (IIV-30)	YP_009010370.1	15/34 (44)	24/34 (70)
Invertebrate iridescent virus 22 (IIV-22)	YP_008357369.1	15/34 (44)	24/34 (70)
Invertebrate iridescent virus 1 (IIV-1; *Tipula* iridescent virus)	P18162.1	15/34 (44)	24/34 (70)
Invertebrate iridescent virus 9 (IIV-9; *Wiseana* iridescent virus)	YP_004732793.1	15/33 (45)	23/33 (69)
Lymphocystis disease virus 1 (LCDV-1)	AHW84100.1	16/33 (48)	24/33 (72)
Invertebrate iridescent virus 25 (IIV-25)	YP_009010611.1	15/33 (45)	23/33 (69)
Lymphocystis disease virus - China (LCDV-C)	YP_025102.1	16/33 (48)	23/33 (69)
Invertebrate iridescent virus 3 (IIV-3)	YP_654586.1	14/34 (41)	24/34 (70)
Invertebrate iridescent virus 31 (IIV-31)	BAL49811.1	16/32 (50)	20/32 (62)
Erythrocytic necrosis virus (ENV)	ALP86597.1	15/33 (45)	22/33 (66)
Invertebrate iridescent virus 6 (IIV-6)	NP_149737.1	15/32 (47)	20/32 (62)

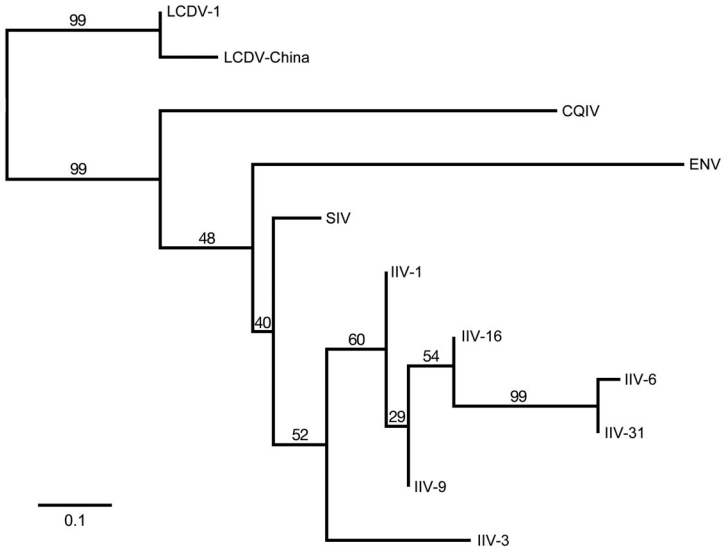

Fig. 6. Phylogenetic tree of the 34 aa region of *Cherax quadricarinatus* iridovirus (CQIV) and iridovirus major capsid proteins (MCPs). Maximum-likelihood analysis using RAxMLGUI with 1000 rapid bootstrap replicates (numbers = bootstrap percentage values). Virus abbreviations are given in Table 1

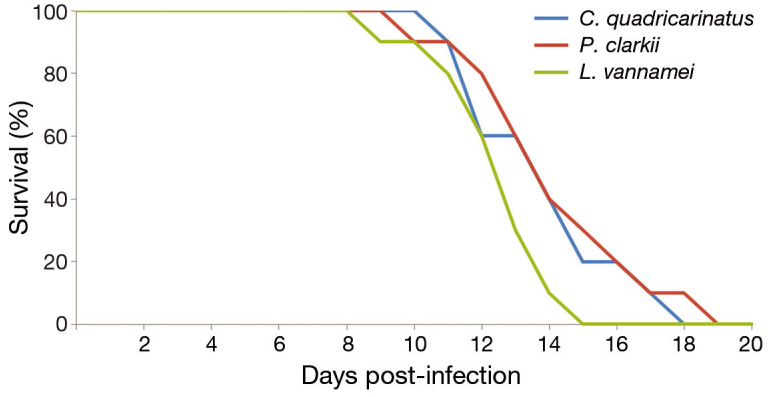

Fig. 7. Survival of crustaceans (*Cherax quadricarinatus*, *Procambarus clarkii*, and *Litopenaeus vannamei*) injected intramuscularly with 2 µl g^{-1} body weight of 10^{-6} dilution of purified *Cherax quadricarinatus* iridovirus

DISCUSSION

Of the 5 genera in the family *Iridoviridae*, members of the genus *Iridovirus* have been identified in diverse invertebrates including arachnids, cephalopods, crustaceans, insects, mollusks, nematodes, and polychaetes, whereas members of the genus *Chloriridovirus* have been identified only in mosquitoes (Williams 2008). Here we report preliminary morphological and genome sequence data on *Cherax quadricarinatus* iridovirus (CQIV), a new iridovirus found in 2014 to be associated with lethargy, anorexia, and mortality in *C. quadricarinatus* farmed in Fujian, China. TEM identified virions exclusively in the cytoplasm of HPT and gill cells of affected crayfish. The virions were icosahedral in shape and ~150 nm in diameter, consistent with other viruses in the family *Iridoviridae*. CQIV particles were also observed at various stages of egression from the plasma membrane and in immediate extracellular spaces, as observed to occur with members of the genus *Ranavirus* (Qin et al. 2003, Chinchar et al. 2011, Ma et al. 2014).

Although iridoviruses have been described in several crustaceans (Federici & Hazard 1975, Leibovitz & Koulish 1989, Lightner &

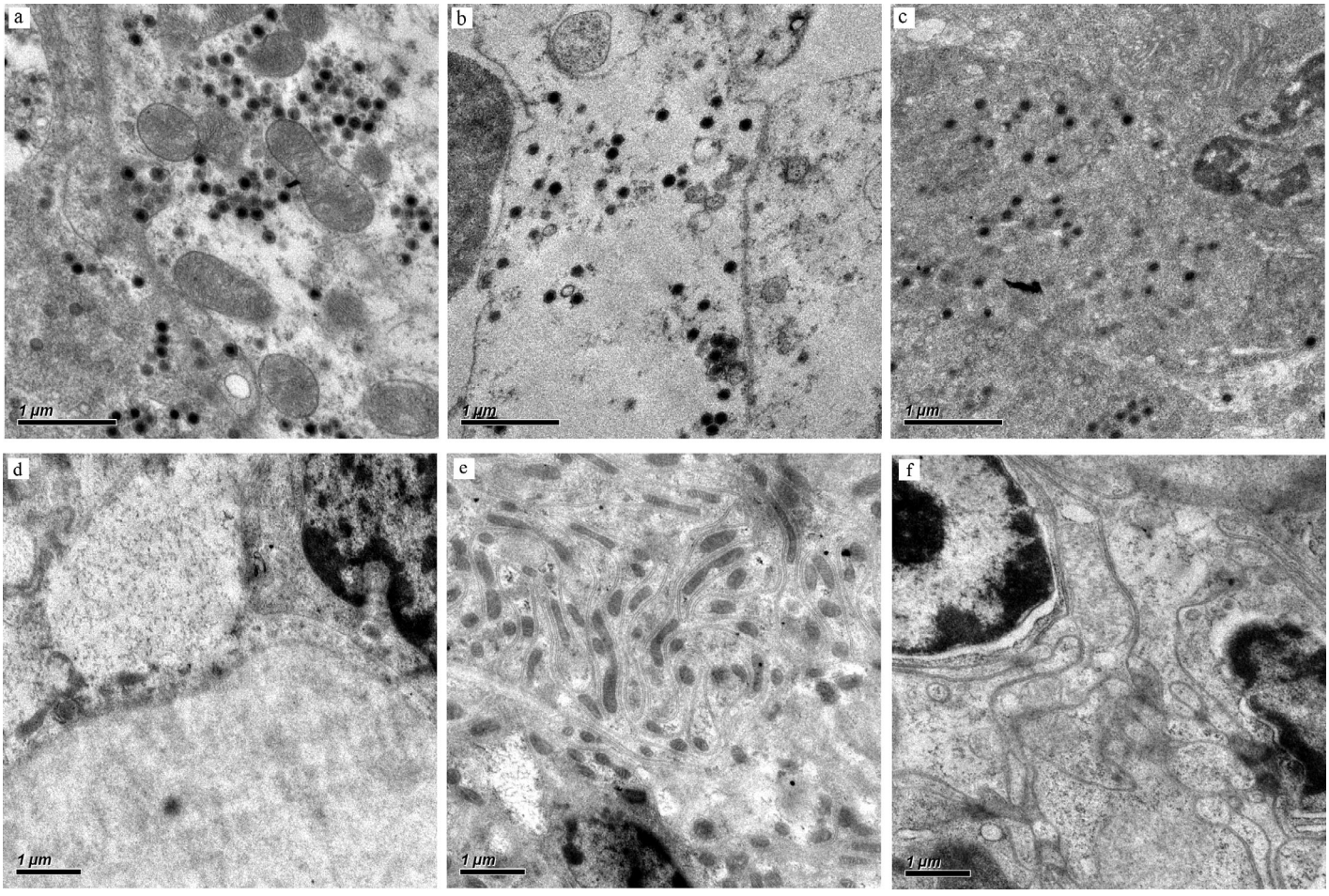

Fig. 8. Transmission electron microscopy of gill tissue of (a,d) *Cherax quadricarinatus*, (b,e) *Procambarus clarkii*, and (c,f) *Litopenaeus vannamei* injected with (a,b,c) purified *C. quadricarinatus* iridovirus or (d,e,f) saline

Redman 1993, Montanie et al. 1993, Tang et al. 2007), information has been generally limited to virus morphology, cytopathology, and histopathology. CQIV particles purified from hemolymph of moribund *C. quadricarinatus* were identified by SDS-PAGE to comprise at least 24 structural proteins ranging from 14 to 120 kDa with the most abundant consistent in mass (~50 kDa) with the MCP of IIVs (Kelly et al. 1979).

Complete genome sequences (190–220 kb in length) are currently available for the iridoviruses IIV-6 (Jakob et al. 2001), IIV-9 (Wong et al. 2011), IIV-22 (Piégu et al. 2013), IIV-25 (Piégu et al. 2014b), IIV-30 (Piégu et al. 2014a), and IIV-31 (Piégu et al. 2014c), as well as the chloriridovirus IIV-3 (Delhon et al. 2006). By digesting DNA isolated from purified virions with various restriction endonucleases and resolving the DNA fragments by agarose gel electrophoresis, the CQIV genome was estimated to be ~150 kb long, thus somewhat shorter than the genomes of other IIVs. However, being rudimentary, this method could have underestimated the CQIV genome length, and its length needs to be determined more accurately by sequence analysis.

To examine the phylogenetic relationship of CQIV to other iridoviruses, a region of the gene encoding the MCP, a protein which has been used to estimate genetic relationships among members of the *Iridoviridae* family (Webby & Kalmakoff 1999, Qin et al. 2003, Do et al. 2005), was amplified by PCR, cloned, and sequenced. BLASTp analysis of the 34 aa MCP fragment encoded in the amplified product showed CQIV to be most closely related to SIV (55% identity), an unclassified iridovirus identified in sergestid shrimp (Tang et al. 2007), and to be slightly less related to other invertebrate iridoviruses (Table 1). The phylogenetic analysis also suggested that CQIV might be sufficiently unrelated to known iridoviruses

to warrant classification into a new genus. However, as some clades on the phylogenetic tree were not well supported as a likely result of the short amino acid sequence analyzed, more genome sequence data will be required to more precisely define the taxonomic relationship of CQIV to other IIVs.

CQIV was confirmed to be pathogenic for *C. quadricarinatus* as well as *Procambarus clarkii* and *Litopenaeus vannamei* in experimental challenge trials. As these represent the most extensively cultured freshwater and marine crustacean species in China, CQIV has significant potential to place the culture of these species at risk. Further studies are thus warranted to clarify the epidemiology and transmission pathways of CQIV to assist in mitigating its disease risks.

Acknowledgements. This work was supported by National Basic Research Program of China (973 Program, 2012CB 114401), China Agriculture Research System (CARS-47), and National Natural Science Foundation of China (No.41376173, No. 41276176).

LITERATURE CITED

Altschul SF, Gish W, Miller W, Myers EW, Lipman DJ (1990) Basic local alignment search tool. J Mol Biol 215:403–410

Anderson JF (1970) An iridescent virus infecting the mosquito *Aedes stimulans.* J Invertebr Pathol 15:219–224

Bächi B, Arber W (1977) Physical mapping of *Bgl*II, *Bam*HI, *Eco*RI, *Hin*dIII and *Pst*I restriction fragments of bacteriophage P1 DNA. Mol Gen Genet 153:311–324

Chinchar V, Hyatt A, Miyazaki T, Williams T (2009) Family *Iridoviridae*: poor viral relations no longer. Curr Top Microbiol Immunol 328:123–170

Chinchar VG, Yu KH, Jancovich JK (2011) The molecular biology of frog virus 3 and other iridoviruses infecting cold-blooded vertebrates. Viruses 3:1959–1985

Comps M (1988) Epizootic diseases of oysters associated with viral infections. Am Fish Soc Spec Publ 18:23–37

Delhon G, Tulman ER, Afonso CL, Lu Z and others (2006) Genome of Invertebrate iridescent virus type 3 (mosquito iridescent virus). J Virol 80:8439–8449

Do JW, Cha SJ, Kim JS, An EJ and others (2005) Phylogenetic analysis of the major capsid protein gene of iridovirus isolates from cultured flounders *Paralichthys olivaceus* in Korea. Dis Aquat Org 64:193–200

Federici BA, Hazard EI (1975) Iridovirus and cytoplasmic polyhedrosis virus in the freshwater daphnid *Simocephalus expinosus.* Nature 254:327–328

Federici BA, Vlak JM, Hamm JJ (1990) Comparative study of virion structure, protein composition and genomic DNA of three ascovirus isolates. J Gen Virol 71:1661–1668

He J, Wang S, Zeng K, Huang Z, Chan SM (2000) Systemic disease caused by an iridovirus-like agent in cultured mandarinfish, *Siniperca chuatsi* (Basilewsky), in China. J Fish Dis 23:219–222

Jakob NJ, Muller K, Bahr U, Darai G (2001) Analysis of the first complete DNA sequence of an invertebrate iridovirus: coding strategy of the genome of Chilo iridescent virus. Virology 286:182–196

Jancovich J, Chinchar V, Hyatt A, Miyazaki T, Williams T, Zhang Q (2012) Family *Iridoviridae*. In: King AMQ, Adams MJ, Carstens EB, Lefkowitz EJ (eds) Virus taxonomy: ninth report of the International Committee on Taxonomy of Viruses. Elsevier Academic Press, San Diego, CA, p 193–210

Kelly D, Ayres M, Lescott T, Robertson J, Happ G (1979) A small iridescent virus (type 29) isolated from *Tenebrio molitor*: a comparison of its proteins and antigens with six other iridescent viruses. J Gen Virol 42:95–105

Laemmli UK (1970) Cleavage of structural proteins during the assembly of the head of bacteriophage T4. Nature 227:680–685

Leibovitz L, Koulish S (1989) A viral disease of the ivory barnacle, *Balanus eburneus*, Gould (Crustacea, Cirripedia). Biol Bull (Woods Hole) 176:301–307

Lightner DV, Redman RM (1993) A putative iridovirus from the penaeid shrimp *Protrachypene precipua* Burkenroad (Crustacea:Decapoda). J Invertebr Pathol 62:107–109

Ma J, Zeng L, Zhou Y, Jiang N and others (2014) Ultrastructural morphogenesis of an amphibian iridovirus isolated from Chinese giant salamander (*Andrias davidianus*). J Comp Pathol 150:325–331

Mao J, Hedrick RP, Chinchar VG (1997) Molecular characterization, sequence analysis, and taxonomic position of newly isolated fish iridoviruses. Virology 229:212–220

Marschang RE, Becher P, Posthaus H, Wild P and others (1999) Isolation and characterization of an iridovirus from Hermann's tortoises (*Testudo hermanni*). Arch Virol 144: 1909–1922

Montanie H, Bonami JR, Comps M (1993) Irido-like virus infection in the crab *Macropipus depurator* L. (Crustacea, Decapoda). J Invertebr Pathol 61:320–322

Piégu B, Guizard S, Spears T, Cruaud C and others (2013) Complete genome sequence of invertebrate iridescent virus 22 isolated from a blackfly larva. J Gen Virol 94: 2112–2116

Piégu B, Guizard S, Spears T, Cruaud C and others (2014a) Complete genome sequence of invertebrate iridovirus IIV30 isolated from the corn earworm, *Helicoverpa zea.* J Invertebr Pathol 116:43–47

Piégu B, Guizard S, Spears T, Cruaud C and others (2014b) Complete genome sequence of invertebrate iridovirus IIV-25 isolated from a blackfly larva. Arch Virol 159: 1181–1185

Piégu B, Guizard S, Yeping T, Cruaud C and others (2014c) Genome sequence of a crustacean iridovirus, IIV31, isolated from the pill bug, *Armadillidium vulgare.* J Gen Virol 95:1585–1590

Qin QW, Chang SF, Ngoh-Lim GH, Gibson-Kueh S, Shi C, Lam TJ (2003) Characterization of a novel ranavirus isolated from grouper *Epinephelus tauvina.* Dis Aquat Org 53:1–9

Silvestro D, Michalak I (2012) raxmlGUI: a graphical front-end for RAxML. Org Divers Evol 12:335–337

Stamatakis A (2014) RAxML Version 8: a tool for phylogenetic analysis and post-analysis of large phylogenies. Bioinformatics 30:1312–1313

Tang KF, Redman RM, Pantoja CR, Groumellec ML, Duraisamy P, Lightner DV (2007) Identification of an iridovirus in *Acetes erythraeus* (Sergestidae) and the development of in situ hybridization and PCR method for

its detection. J Invertebr Pathol 96:255–260

Webby RJ, Kalmakoff J (1999) Comparison of the major capsid protein genes, terminal redundancies, and DNA-DNA homologies of two New Zealand iridoviruses. Virus Res 59:179–189

Weissenberg R (1965) Fifty years of research on the lymphocystis virus disease of fishes (1914 1964). Ann NY Acad Sci 126:362–374

Williams T (2008) Natural invertebrate hosts of iridoviruses (Iridoviridae). Neotrop Entomol 37:615–632

Williams T, Barbosa-Solomieu V, Chinchar VG (2005) A decade of advances in iridovirus research. Adv Virus Res 65:173–248

Wong CK, Young VL, Kleffmann T, Ward VK (2011) Genomic and proteomic analysis of invertebrate iridovirus type 9. J Virol 85:7900–7911

Editorial responsibility: Jeff Cowley, Brisbane, Queensland, Australia

Submitted: October 12, 2015; Accepted: April 14, 2016
Proofs received from author(s): June 12, 2016